

Information Theoretic Structured Generative Modeling

Bo Hu¹, Shujian Yu^{2,3}, José C. Príncipe¹

¹ University of Florida, Gainesville, FL 32611, USA
hubo@ufl.edu; principe@cnel.ufl.edu

² UiT - The Arctic University of Norway, 9037 Tromsø, Norway

³ Xi'an Jiaotong University, Xi'an 710049, Shaanxi, China
yusj9011@gmail.com

October 13, 2021

Abstract

Rényi's information provides a theoretical foundation for tractable and data-efficient non-parametric density estimation, based on pair-wise evaluations in a reproducing kernel Hilbert space (RKHS). This paper extends this framework to parametric probabilistic modeling, motivated by the fact that Rényi's information can be estimated in closed-form for Gaussian mixtures. Based on this special connection, a novel generative model framework called the structured generative model (SGM) is proposed that makes straightforward optimization possible, because costs are scale-invariant, avoiding high gradient variance while imposing less restrictions on absolute continuity, which is a huge advantage in parametric information theoretic optimization. The implementation employs a single neural network driven by an orthonormal input appended to a single white noise source adapted to learn an infinite Gaussian mixture model (IMoG), which provides an empirically tractable model distribution in low dimensions. To train SGM, we provide three novel variational cost functions, based on Rényi's second-order entropy and divergence, to implement minimization of cross-entropy, minimization of variational representations of f -divergence, and maximization of the evidence lower bound (conditional probability). We test the framework for estimation of mutual information and compare the results with the mutual information neural estimation (MINE), for density estimation, for conditional probability estimation in Markov models as well as for training adversarial networks. Our preliminary results show that SGM significantly improves MINE estimation in terms of data efficiency and variance, conventional and variational Gaussian mixture models, as well as the performance of generative adversarial networks.

1 Introduction

The traditional information descriptors in probability spaces are Shannon's entropy, Mutual Information, and the Kullback–Leibler divergence (relative entropy). Since the probability density function of the data in machine learning is often unknown, applying these descriptors requires well-behaved estimators or approximations. The objective of information theoretic

learning (ITL) is to provide a clear and theoretically supported view of probabilistic modeling algorithms. There are basically two different avenues in the literature: non-parametric estimators and parametric estimators. Rényi’s second-order entropy and divergence have been broadly used for designing non-parametric estimators [1, 2] following the principle of sample-based pair-wise evaluations in reproducing kernel Hilbert space (RKHS). The main difficulty of this non-parametric framework is its dependence on a free parameter that yields a bias. If the bias can be tolerated (e.g. optimization of ITL cost functions), its appeal is interpretability, data efficiency, and good performance [3].

The other avenue optimizes a universal parametric model to estimate the ITL descriptors, which usually follows three types of principles: minimizing cross-entropy [4, 5], minimizing variational representations of f -divergence [6, 7, 8], and maximizing the evidence lower bound (ELBO) [9, 10, 11]. For example, minimization of cross-entropy, which is simple to implement from the data distributions, yields a model that is an upper bound for the data entropy [4, 5]. Solving variational representations of f -divergence based on a function of the probability ratio $p(x)/q(x)$ quantifies the divergence between two distributions as an upper bound of the model mapping [6, 7]. Recently, generative adversarial networks (GANs) [8] take this approach with one network approximating f -divergence and another network producing an intractable model distribution to minimize the approximated f -divergence [12, 13]. In variational inference, if direct optimization over cross-entropy is difficult, ELBO introduces a latent variable with conditional probabilities to optimize the parameters of an underlying model that has a simpler structure [9].

However, experience has shown that optimizing all these costs is a challenging task. The main reason is that Shannon’s cross-entropy or Kullback–Leibler divergence require absolute continuity of two Lebesgue measures $Q \gg P$, which is highly restrictive during adaptation of any parameterized model that yields the distribution. Without this condition the bounds do not hold. Secondly, in order to avoid estimating the nonlinear $\log q(x)$, the asymptotic equipartition property (AEP) is normally utilized [14], which is not data efficient. Thirdly, the ultimate task is to produce a valid probability distribution, which requires constrained optimization methodologies. All three aspects also create high variance in the gradient and forbid the application of simple optimization techniques. The field conventionally uses expectation maximization (EM) [5], stochastic approximation [15], or what is also called “reparameterization tricks” [16].

The main contribution of this paper is to propose a unified new set of information theoretic cost functions based on the theory of Rényi’s entropy and divergence [17] that improves these three issues. Rényi’s entropy and the corresponding divergence are related to the special case of f -divergence when the convex function f is taken to be a polynomial. We derive three variational forms for Rényi’s second-order entropy, divergence, and conditional entropy that corresponds to the three mentioned principles. The important property of Rényi’s information as opposed to Shannon is that the log is outside of the integral, which simplifies the estimation [1] and provides a closed-form solution for mixture of Gaussian [18], which dramatically simplifies the computation for the versatile class of generalized Gaussian mixture models. The second contribution is to propose a new generative model framework called the structured generative model (SGM) for modeling distributions or conditional distributions by approximating local sample densities by their mean and variance, assuming a

versatile generalized Gaussian mixture model. SGM uses a single neural network to produce an infinite mixture of Gaussian (IMoG) that can be trained efficiently and robustly by the newly proposed cost through gradient methods. Compared to conventional methods, it can produce an empirically tractable probability distribution and hugely improves performance with much smaller bias and less variance for the class of IMoG problems. To further demonstrate the superiority of our cost function, we compare with MINE estimators, we show its versatility by estimating conditional probabilities, and we also show an example of the newly proposed variational divergence form to train a GAN. Under the proposed framework, the discriminator network will produce a probability ratio, which can have broad applications such as out-of-distribution (OOD) detection [19].

2 Background

We start with an introduction of cross-entropy, f -divergence, and a short discussion about Gaussian mixture models (GMM) and generative adversarial networks (GAN) from the perspective of ITL. Then we introduce Rényi's entropy and divergence. Throughout the paper, we assume that the density functions exist and are Lebesgue measurable. We use the definition of differential entropy for the continuous random variables.

Cross-entropy and GMM: Let a density function $q(x)$ be given. Taking the expectation of $-\log q(x)$ over $p(x)$ yields the cross-entropy $\text{CE}(p, q)$, which satisfies

$$\text{CE}(p, q) = - \int_{\mathcal{X}} p(x) \log q(x) = - \int_{\mathcal{X}} p(x) \log p(x) + \text{KL}(p||q) \geq - \int_{\mathcal{X}} p(x) \log p(x) = H(p). \quad (1)$$

Thus, minimizing $\text{CE}(p, q)$ yields $H(p)$, and the tightness of the bounds depends directly on $\text{KL}(p||q)$, which is a problem. It is well-known that Gaussian mixture models maximizes the log likelihood of data, but it can also be formulated as minimizing the cross-entropy. Let the model density be $g_{\theta}(x) = \sum_{i=1}^N w_i \mathcal{N}(x - m_i, A_i)$ with mean values $\{m_1, \dots, m_N\}$ and covariance matrices $\{A_1, \dots, A_N\}$. By (1), the cross-entropy satisfies $\text{CE}(p, g_{\theta}) = - \int_{\mathcal{X}} p(x) \log \sum_{i=1}^N w_i \mathcal{N}(x - m_i, A_i) d\mu \geq H(p)$. We write $g_{\theta}(x, z = i) = w_i \mathcal{N}(x - m_i, A_i)$. Since $\partial \text{CE}(p, g_{\theta}) / \partial \theta = 0$ does not have a closed-form solution, expectation maximization (EM) and variational inference optimize an upper bound of $\text{CE}(p, g_{\theta})$:

$$\begin{aligned} \text{CE}(p, g_{\theta}) &= \int_{\mathcal{X}} \int_{\mathcal{Z}} p(x) \frac{g_{\theta}(x, z)}{\int_{\mathcal{Z}} g_{\theta}(x, z) d\mu} \log \frac{g_{\theta}(x, z)}{\int_{\mathcal{Z}} g_{\theta}(x, z) d\mu} d\mu d\mu - \int_{\mathcal{X}} \int_{\mathcal{Z}} p(x) \frac{g_{\theta}(x, z) \log g_{\theta}(x, z)}{\int_{\mathcal{Z}} g_{\theta}(x, z) d\mu} d\mu d\mu \\ &\leq - \int_{\mathcal{X}} \int_{\mathcal{Z}} p(x) (g_{\theta}(x, z) / g_{\theta}(x)) \log g_{\theta}(x, z) d\mu = \text{CE}(p(x) g_{\theta}(x, z) / g_{\theta}(x), g_{\theta}(x, z)). \end{aligned} \quad (2)$$

Ideally, the upper bound is minimized when $p(x) g_{\theta}(x, z) / g_{\theta}(x) = g_{\theta}(x, z)$, i.e., $g_{\theta}(x) = p(x)$, which yields the same solution as minimizing $\text{CE}(p, g_{\theta})$. EM iteratively updates $\theta^{\text{new}} = \max_{\theta} \text{CE}(p(x) g_{\theta'}(x, z) / g_{\theta'}(x), g_{\theta}(x, z))$. Gradient methods can also be used [5, 20]. However, the condition for this upper bound to hold is very restrictive. Suppose there exists x such that $p(x) > 0$ and $g_{\theta}(x) = 0$, it is easy to show that $\text{CE}(p, g_{\theta}) \rightarrow \infty$. On the other hand, the responsibility $g_{\theta}(x, z) / g_{\theta}(x)$ is taken to be finite such that the RHS has finite values. In this case, the bound no longer exists.

f -divergence and GAN: Another important branch of costs is the f -divergence. Given a convex function f with $f(1) = 0$, f -divergence has the form $D_f(p||q) = \int_{\mathcal{X}} q(x)f(p(x)/q(x))d\mu$ that evaluates a “distance” between two distributions. A variational form of $D_f(p||q)$ takes the convex conjugate of f [21], which becomes [13]:

$$D_f(p||q) \geq \sup_{T \in \mathcal{T}} \left(\int T(x)p(x)d\mu - \int f^*(T(x))q(x)d\mu \right) = \sup_{T \in \mathcal{T}} (\mathbb{E}_p[T(x)] - \mathbb{E}_q[f^*(T(x))]), \quad (3)$$

where \mathcal{T} is an arbitrary class of functions $T : \mathcal{X} \rightarrow \mathbb{R}$. The bound is tight when $T_0(x) = f'(p(x)/q(x))$. Although T_0 is written in the form of $p(x)/q(x)$, the absolute continuity condition also depends on the choice of f .

Any universal parametric model such as kernel functions [6, 7] or neural networks [22] can be used to approximate T by maximizing the lower bound. GAN uses a discriminator network to approximate T , and a generator network to produce an intractable model distribution g_θ that minimizes the approximated f -divergence [12, 13]. The most obvious downside is that g_θ is intractable. Secondly, although T_θ should approach $T_0(x)$ related to the probability ratio, there is no guarantee in GAN.

Rényi’s entropy and divergence: Finally, we mention Rényi’s entropy and divergence of order α

$$H_\alpha(p) = \frac{1}{1-\alpha} \log \int_{\mathcal{X}} p^\alpha(x)d\mu, \quad D_\alpha(p||q) = \frac{1}{1-\alpha} \log \int_{\mathcal{X}} p^\alpha(x)q^{1-\alpha}(x)d\mu. \quad (4)$$

Rényi’s divergence is related to the special case of (3) when f is chosen to be a polynomial. The existence of $D_\alpha(p||q)$ requires $Q \gg P$ for all $\alpha \geq 1$. When α is 2, Rényi’s second-order divergence matches the χ^2 -divergence. Rényi’s second-order entropy and divergence are the foundations of non-parametric density estimators based on sample-based pair-wise evaluations and the theory of RKHS [1]. This paper further expands this idea.

3 Variational Costs in Rényi’s Forms

Now we introduce two new variational forms $J_p(T)$ and $J_{p,q}(T)$, which accepts upper bound related to Rényi’s second-order entropy $H_2(P)$ and second-order divergence $D_2(P||Q)$.

Variational form of Rényi’s second-order entropy. Similar to the cross-entropy, we introduce a functional $J_p(T)$ that has the following form

$$J_p(T) = \int_{\mathcal{X}} p(x)T(x)d\mu / \left(\int_{\mathcal{X}} T^2(x)d\mu \right)^{\frac{1}{2}} = \mathbb{E}_p[T(x)] / \left(\int_{\mathcal{X}} T^2(x)d\mu \right)^{\frac{1}{2}}. \quad (5)$$

where the set \mathcal{T} contains any non-negative measurable function with $\int_{\mathcal{X}} T^2(x)d\mu > 0$. For simplicity, we write the inner product $\int_{\mathcal{X}} p(x)T(x)d\mu := \langle p, T \rangle$, the norm $\int_{\mathcal{X}} p^2(x)d\mu = \langle p, p \rangle$, and $\int_{\mathcal{X}} T^2(x)d\mu = \langle T, T \rangle$. By Cauchy-Schwarz inequality, we have $\langle p, T \rangle \leq \sqrt{\langle p, p \rangle \langle T, T \rangle}$. It follows that $J_p(T) = \langle p, T \rangle / \sqrt{\langle T, T \rangle} \leq \sqrt{\langle p, p \rangle}$. Therefore we proved that

$$\sup_{T \in \mathcal{T}} J_p(T) = \left(\int_{\mathcal{X}} p^2(x)d\mu \right)^{\frac{1}{2}}. \quad (6)$$

There are two important conclusions: first, the upper bound only depends the data, and second the solution is $T_0(x) = \beta p(x)$ with β taken to be any arbitrary positive scalar. The function T can be approximated by any parametric model.

Variational form of Rényi’s second-order divergence. Following a similar idea, we introduce a functional $J_{p,q}(T)$ for Rényi’s second-order divergence, written as

$$J_{p,q}(T) = \int_{\mathcal{X}} p(x)T(x)d\mu / (\int_{\mathcal{X}} q(x)T^2(x)d\mu)^{\frac{1}{2}} = \mathbb{E}_p[T(x)] / (\mathbb{E}_q[T^2(x)])^{\frac{1}{2}}. \quad (7)$$

Similarly, applying Cauchy-Schwartz inequality

$$J_{p,q}(T) = \langle p(x)/\sqrt{q(x)}, T\sqrt{q(x)} \rangle / \langle T\sqrt{q(x)}, T\sqrt{q(x)} \rangle^{\frac{1}{2}} \leq \langle p(x)/\sqrt{q(x)}, p(x)/\sqrt{q(x)} \rangle^{\frac{1}{2}}. \quad (8)$$

Therefore we proved that the upper bound of $J_{p,q}(T)$ exists and

$$\sup_{T \in \mathcal{T}} J_{p,q}(T) = (\int_{\mathcal{X}} p^2(x)/q(x)d\mu)^{\frac{1}{2}}. \quad (9)$$

The supremum is attained as $T_0(x) = \beta p(x)/q(x)$, which is a scaled value of the probability ratio. Combining with (4), it can be shown that the upper bounds of $J_p(T)$ and $J_{p,q}(T)$ are related to Rényi’s second-order entropy and divergence as $H_2(P) = -2 \log \sup_{T \in \mathcal{T}} J_p(T)$ and $D_2(P||Q) = -2 \log \sup_{T \in \mathcal{T}} J_{p,q}(T)$.

The advantages of such formulations is two folds: **(a) Scale-invariance.** Both $J_p(T)$ and $J_{p,q}(T)$ are scale-invariant to T . For $J_p(T)$, the function T does not need to satisfy $\int_{\mathcal{X}} T_0(x)d\mu = 1$, which matches Rényi’s definition of the a generalized probability distribution [23]. This avoids the annoying normalizing constant. **(b) Less restrictions on absolute continuity.** The existence of $J_p(T)$ requires only $\int_{\mathcal{X}} T^2(x)d\mu > 0$, which is a much milder condition than what is shown in Section 2.

4 Training Models with Rényi’s Variational Costs

Now we show how $J_p(T)$ and $J_{p,q}(T)$ can be employed for model training. First, optimizing $J_{p,q}(T)$ shares the same procedure as optimizing any variational form of f -divergence [6, 7, 22]. It can also train a generative adversarial network with the discriminator network producing the probability ratio. Optimizing $J_p(T)$ is challenging because the normalizing term $\int_{\mathcal{X}} T^2(x)d\mu$. One unwise choice is to impose a uniform distribution such that $\int_{\mathcal{X}} T^2(x)d\mu = \mathbb{E}_u[T^2(x)]/Z$. This is not practical since the support of the data distribution may be unknown. In this section, we show that if $T(x)$ is a mixture of Gaussian (MoG) or an infinite mixture of Gaussian (IMoG), the term $\int_{\mathcal{X}} T^2(x)d\mu$ will have a closed-form solution, but of course also inherit some of their limitations.

4.1 Pair-wise Properties of MoG

To distinguish from the parameters of neural networks θ , we use φ as the parameters of an MoG. In the Bayesian setting, it can be given by a distribution. We first start with the MoG with finite components.

Finite case. Suppose $\varphi = \{\varphi_1, \dots, \varphi_N\}$ defines a MoG with each $\varphi_i = \{w_i, m_i, A_i\}$. The model density function has the form $T_\varphi(x) = \sum_{i=1}^N w_i \mathcal{N}(x - m_i, A_i)$. We do not require $\sum_{i=1}^N w_i = 1$ but only require each w_i to be non-negative. It's easy to show that

$$\begin{aligned} \int_{\mathcal{X}} T_\varphi^2(x) d\mu &= \int_{\mathcal{X}} \sum_{i=1}^N \sum_{j=1}^N w_i w_j \mathcal{N}(x - m_i, A_i) \mathcal{N}(x - m_j, A_j) d\mu \\ &= \sum_{i=1}^N \sum_{j=1}^N w_i w_j \mathcal{N}(m_i - m_j, A_i + A_j), \end{aligned} \quad (10)$$

given $\int_{\mathcal{X}} \mathcal{N}(x - m_i, A_i) \mathcal{N}(x - m_j, A_j) d\mu = \mathcal{N}(m_i - m_j, A_i + A_j)$. This term is fully determined by φ with a closed-form solution based on pair-wise relations [18].

Infinite Gaussian mixtures. To further increase the generalization capability of this approach, we show that the same conclusion holds for an IMoG in a Bayesian setting, where φ is determined by an arbitrary distribution P_φ . Thus the model density has the form $T_\varphi(x) = \mathbb{E}_{\varphi \sim P_\varphi} [\mathbf{w} \mathcal{N}(x - \mathbf{m}, \mathbf{A})]$. Similarly it can be shown that

$$\int_{\mathcal{X}} T_\varphi^2(x) d\mu = \mathbb{E}_{\varphi_1 \sim P_\varphi, \varphi_2 \sim P_\varphi} [\mathbf{w}_1 \mathbf{w}_2 \mathcal{N}(\mathbf{m}_1 - \mathbf{m}_2, \mathbf{A}_1 + \mathbf{A}_2)]. \quad (11)$$

In this form, the distribution P_φ can either be a prior distribution such as a Dirichlet process or a generative model. It should also be stated that if P_φ is given by a generative model, we should still impose constraint on the generative model to control its model complexity because only finite number of samples are given [6]. Now we propose a generative approach based on a neural network that produces the model density $T_\varphi(x)$. While imposing a MoG can introduce a bias [5], but the advantage of controlling the variance with a model is very appealing and surpasses the former.

4.2 Structured Generative Models

Similar to GAN, we impose two types of network input \mathbf{z} and \mathbf{c} . Let the size of the orthogonal vectors be N , which is the space dimension. We define $z_i(j) = \begin{cases} 1 & \text{if } i = j \\ 0 & \text{if } i \neq j \end{cases}$.

For $1 \leq i \leq N$, we write the vector as $z_i = [z_i(1), z_i(2), \dots, z_i(N)]^\top$. The orthonormal set is given by $\{z_1, z_2, \dots, z_N\}$. Let an uniformly sampled random noise $\mathbf{c} \sim U(0, 1)$ be given. We call the combination of the elements in the orthonormal set and the noise \mathbf{c} the scanning vectors, whose role is to span the sample space to quantify local structures. The output of the neural net defines P_φ . With z_i and \mathbf{c} as the input, we denote the output of the neural net as $\{f_\theta^{(w)}(z_i, \mathbf{c}), f_\theta^{(m)}(z_i, \mathbf{c}), f_\theta^{(A)}(z_i, \mathbf{c})\}$. The model density function has the form

$$g_\theta(x) = \mathbb{E}_{\mathbf{c}} \left[\frac{1}{N} \sum_{i=1}^N f_\theta^{(w)}(z_i, \mathbf{c}) \mathcal{N}(x - f_\theta^{(m)}(z_i, \mathbf{c}), f_\theta^{(A)}(z_i, \mathbf{c})) \right]. \quad (12)$$

Writing $w_i(\mathbf{c}) = f_\theta^{(w)}(z_i, \mathbf{c})$, $m_i(\mathbf{c}) = f_\theta^{(m)}(z_i, \mathbf{c})$, $A_i(\mathbf{c}) = f_\theta^{(A)}(z_i, \mathbf{c})$. With (23), we have

$$\int_{\mathcal{X}} g_\theta^2(x) d\mu = \mathbb{E}_{\mathbf{c}_1, \mathbf{c}_2} [w_i(\mathbf{c}_1) w_j(\mathbf{c}_2) \mathcal{N}(m_i(\mathbf{c}_1) - m_j(\mathbf{c}_2), A_i(\mathbf{c}_1) + A_j(\mathbf{c}_2))], \quad (13)$$

which is fully defined by P_φ , irrelevant to the data distribution and avoids an empirical estimation over \mathcal{X} . The optimization problem can be written as

$$\text{maximize}_{g_\theta} J_p(g_\theta) = \mathbb{E}_p[g_\theta(x)] / \left(\int_{\mathcal{X}} g_\theta^2(x) d\mu \right)^{\frac{1}{2}}. \quad (14)$$

The added advantage is that the model can be trained efficiently by gradient ascent. The upper bound of the cost function is given by (6) and the bound is tight if $g_\theta(x) = p(x)$. We call this approach the structured generative model (SGM). SGM can be said to have the following advantages:

- Optimizing SGM produces a generalized probability distribution that does not require the normalizing constant. And its value exists even when g_θ does not cover the entire support of p . These make a distinguishable difference and are an improvement from the traditional methods.
- SGM can be optimized very easily by gradient ascent. While algorithms such as EM has a weak optimality guarantee, the SGM optimization is theoretically justified since the SGM cost is upper bounded by (6). Unlike VBGMM, SGM will not have a severe bias issue.
- Compared to GAN, SGM does not have an extra auxiliary model because of the powerful combination of the neural network and the cost function. The model produces an empirically tractable density function. Compared to GMM and VBGMM, we utilize an universal mapper and it is not necessary to specify the responsibility.

Variance reduction. One difficulty for optimizing directly with such a cost is the variance of the gradient. The variance in the gradient of $J_p(g_\theta)$ can be reduced in a procedure introduced in [24]. Write $c_\theta = \mathbb{E}_p[g_\theta(x)]$ and $v_\theta = \int_{\mathcal{X}} g_\theta^2(x) d\mu$, the gradient of $J_p(g_\theta)$ has the form $\frac{\partial J_p(g_\theta)}{\partial \theta} = \frac{\partial c_\theta}{\partial \theta} / \sqrt{v_\theta} - \frac{1}{2} (c_\theta \frac{\partial v_\theta}{\partial \theta}) / \sqrt{v_\theta^3}$. Therefore c_θ and v_θ can be estimated adaptively over time. At iteration t , suppose the adaptive filters produce \tilde{c}_t and \tilde{v}_t . Suppose the empirical estimations based on θ_t are \hat{c}_{θ_t} and \hat{v}_{θ_t} . The gradient can be constructed by $\frac{\partial J_p(g_{\theta_t})}{\partial \theta_t} \approx \frac{\partial \hat{c}_{\theta_t}}{\partial \theta_t} / \sqrt{\tilde{v}_t} - \frac{1}{2} (\tilde{c}_t \frac{\partial \hat{v}_{\theta_t}}{\partial \theta_t}) / \sqrt{\tilde{v}_t^3}$. This trick has been also applies to the divergence cost (7).

4.3 Modeling Conditional Probabilities

Furthermore, SGM is capable of modeling conditional probabilities. We first derive the corresponding variational form. Let a conditional probability $p(y|x)$ and an arbitrary $p(x)$ be given. We define

$$J_{Y|X}(T) = \int_{\mathcal{X}} \int_{\mathcal{Y}} T(y|x) p(y|x) p(x) d\mu d\mu / \left(\int_{\mathcal{X}} \int_{\mathcal{Y}} T^2(y|x) p(x) d\mu d\mu \right)^{\frac{1}{2}}. \quad (15)$$

Observe that its upper bound is

$$\begin{aligned} J_{Y|X}(T) &= \langle T(y|x) \sqrt{p(x)}, p_\theta(y|x) \sqrt{p(x)} \rangle_{\mathcal{X} \times \mathcal{Y}} / \langle T(y|x) \sqrt{p(x)}, T(y|x) \sqrt{p(x)} \rangle_{\mathcal{X} \times \mathcal{Y}}^{1/2} \\ &\leq \left(\int_{\mathcal{X}} \int_{\mathcal{Y}} p^2(y|x) p(x) d\mu d\mu \right)^{\frac{1}{2}}. \end{aligned} \quad (16)$$

The RHS of (16) is related to Rényi’s definition of conditional entropy [23] as $H_2(Y|X) = -2 \log[\sup_{T \in \mathcal{T}} J_{Y|X}(T)]$. The corresponding solution is $T_0(x|y) = p(y|x)$. To use $J_{Y|X}(T)$ as a cost function for SGM, we assume that $T_0(y|x)$ is approximated by a neural network $g_\theta(y|x)$ by maximizing the lower bound. With any given x , the network output $g_\theta(y|x)$ defines an IMoG for the variable y . Let the network output be $\{w_i(\mathbf{c}; x), m_i(\mathbf{c}; x), A_i(\mathbf{c}; x)\}$, it follows that

$$\int_{\mathcal{Y}} g_\theta^2(y|x) p(x) d\mu = \mathbb{E}_{\mathbf{c}_1, \mathbf{c}_2, x} [w_i(\mathbf{c}_1; x) w_j(\mathbf{c}_2; x) \mathcal{N}(m_i(\mathbf{c}_1; x) - m_j(\mathbf{c}_2; x), A_i(\mathbf{c}_1; x) + A_j(\mathbf{c}_2; x))], \quad (17)$$

which has very little difference from the implementation in 4.2. Then we maximize $J_{Y|X}(g_\theta)$.

Relation to ELBO. We claim that the bound derived in (16) can be formulated as ELBO. Simply substituting y by z and $T(y|x)$ by $T(z)$, the cost $J_{Y|X}$ can be rewritten as

$$\int_{\mathcal{X}} \int_{\mathcal{Z}} T(z) p(z|x) p(x) d\mu d\mu / (\int_{\mathcal{Z}} T^2(z) d\mu)^{\frac{1}{2}}. \quad (18)$$

Comparing with ELBO $L(x) = \int_{\mathcal{Z}} T(z) \log(p(z|x)p(x)) d\mu - \int_{\mathcal{Z}} T(z) \log T(z) d\mu$ and

$$\int_{\mathcal{X}} L(x) p(x) d\mu = \int_{\mathcal{X}} \int_{\mathcal{Z}} p(x) T(z) (\log p(z|x)p(x)) d\mu d\mu - \int_{\mathcal{Z}} T(z) \log T(z) d\mu, \quad (19)$$

it is easy to see both (18) and (19) are determined only by $p(x)$, $p(x, z)$ and $T(z)$. Thus we state that they serve the same purpose. The difference is that we do not need to ignore the denominator in (18) and $T(z)$ does not have to be normalized, which can have a great advantage compared to ELBO.

Relation to mutual information. For mutual information, we define

$$\hat{I}(X; Y) = 2 \log [(\int_{\mathcal{X}} \int_{\mathcal{Y}} p^2(y|x) p(x) d\mu d\mu)^{\frac{1}{2}} / (\int_{\mathcal{X}} p^2(y) d\mu)^{\frac{1}{2}}] = H_2(Y) - H_2(Y|X). \quad (20)$$

It’s easy to verify that $\hat{I}(X; Y) \rightarrow 0$ if X and Y are mutual independent. Thus $\hat{I}(X; Y)$ also characterizes the gain of information about Y when observing X . Suppose $p(y)$ is given, then (20) can be rewritten as $\hat{I}(X; Y) = H_2(Y) + 2 \log[\sup J_{Y|X}(T)]$. Thus we state that by maximizing $J_{Y|X}(T)$, we’re also maximizing a lower bound of a mutual information variation $\hat{I}(X; Y)$.

5 Experiments

We show our experiments in two folds. First, we show how the proposed cost functions and SGM provides new opportunities to train a neural network, such as training a mutual information estimator and a GAN. Secondly, we show the powerful SGM for density estimation and how it differs and improves the conventional GMM and VBGMM.

5.1 Training Neural Networks with Divergence

SGM as a mutual information (MI) estimator. We demonstrate our methods by comparing the performance of estimating MI: (a) SGM density estimator producing the quadratic

mutual information (QMI) $I_Q = -\log_2 \langle p(x, y), p(x)p(y) \rangle + \frac{1}{2} \log_2 \langle p(x)p(y), p(x)p(y) \rangle + \frac{1}{2} \log_2 \langle p(x, y), p(x, y) \rangle$ [1]; (b) Mutual information neural estimation (MINE) [25] producing Shannon’s mutual information; (c) Training the same mapper as MINE with our proposed variational cost $J_{p,q}(T_\theta)$, which yields MI with Rényi’s second-order divergence (Rényi’s MI).

To estimate I_Q with SGM, we first construct the probability ratio of the model $r_\theta(x, y) = \frac{g_\theta(x, y)}{g_\theta(x)g_\theta(y)}$. We define a function of the probability ratio that evaluates MI of the model given data as $\hat{I}_Q(r_\theta) = -\frac{1}{2} \log_2 \left(\frac{\mathbb{E}_{P_X P_Y}[r_\theta(x, y)]}{\mathbb{E}_{P_{XY}}[r_\theta(x, y)]} \right)$. It can be verified $\hat{I}(r_\theta)$ is an unbiased estimator of I_Q as $r_\theta \rightarrow \frac{p(x, y)}{p(x)p(y)}$. Each term in $\hat{I}_Q(r_\theta)$ is a byproduct from optimization.

We generate a mixture distribution with 20 centers uniformly sampled from 0.2 to 0.8 in 2D space. We assign each center to a Gaussian distribution with diagonal covariance matrices from $U(0.0001, 0.002)$. We sample the weighting factor from $U(0.5, 1.5)$. We set $N = 300$ across the experiments.

We test three approaches for the MoG example as before and estimate the mutual information between two dimensions. Figure 1a shows both our approaches are far more stable than MINE which will diverge for small number of samples. Even with variance reduction, MINE suffers from a large variance that cannot be ignored. We compute the ground truth of QMI through (23) and SGM matches the exact value with 5k samples. Rényi’s MI also converges at the same rate, but does not converge to the same value because it uses Rényi’s divergence, instead of QMI, which is a Cauchy-Schwarz divergence [26] estimated with Rényi’s second-order entropy. This also shows that the proposed cost can be applied to any neural network. MINE with enough samples also converges to Shannon’s mutual information but with a high variance. So these proposed estimators are much more well behaved and data efficient to estimate MI, outperforming MINE.

To show the scalability to high dimensions, we generate MoG in high dimensions and compare MINE with optimizing $J_{p,q}(T_\theta)$, shown as Figure 1b. This shows our new cost has the same performance with less variance, but much more stable when only a limited number of samples are accessible, as demonstrated in Figure 1a.

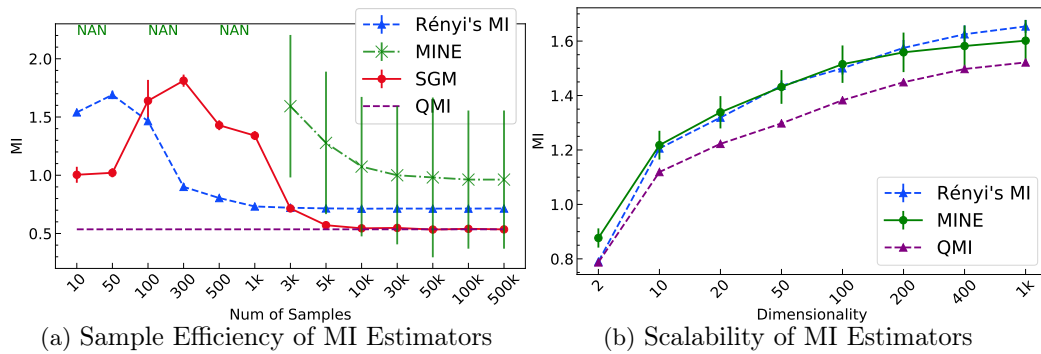


Figure 1: Performance of MI estimators. (a) shows both SGM and optimizing $J_{p,q}(T_\theta)$ shows a better stability and lower variance than MINE, where MINE will diverge (producing “NaN”) for small number of samples. Three approaches converge to Rényi’s second-order MI, Shannon’s MI and QMI respectively. (b) shows that optimizing $J_{p,q}(T_\theta)$ also scales up to high dimensions with a lower variance. As we decrease the training samples for MINE, it will no longer converge.

A new approach to train a GAN. We show the possibility of using $J_{p,q}(T)$ to train a GAN. As stated, the corresponding solution of optimizing a variational form of divergence yields a function of probability ratio, which is rarely addressed in the GAN literature. Let $T_\theta : \mathcal{X} \rightarrow \mathbb{R}$ be the discriminator network and g_θ be the generator network, we formulate the optimization problem as

$$\min_{g_\theta} \max_{T_\theta} J_{g_\theta, p}(T_\theta) = \mathbb{E}_{g_\theta}[T_\theta(x)] / (\mathbb{E}_p[T_\theta^2(x)])^{\frac{1}{2}}. \quad (21)$$

For each fixed g_θ , the corresponding optimal solution of T_θ is $T_0(x) = \beta g_\theta(x) / p(x)$. Ideally, we should obtain $T_0(x) = 0$ for any $x \sim p$.

We train a conventional GAN on the Fashion MNIST. The generated samples are shown as Figure 2a. Figure 2b shows the false positive and false negatives with a threshold of 10^{-2} , which shows the exemplars closer to the boundary. Figure 2c shows the discriminator network output for the Fashion MNIST test set. Then we apply the same discriminator network to the test set of MNIST, producing Figure 2d, where the network produces 0 for in-distribution samples and 1 for out-of-distribution (OOD) samples. We compare our approach with baselines mentioned in [27], including maximum class probability [19], entropy, Mahalanobis distance [28], likelihood ratio [27]. Additionally, we also compare with two state-of-the-art methods based on variational information bottleneck (VIB) [29] and nonlinear information bottleneck (NIB) [30], respectively. In terms of metrics, we use the area under ROC curve (AUROC \uparrow), the area under precision-recall curve (AUPRC \uparrow), and the false positive rate at 80% true positive rate (FPR80 \downarrow). The quantitative results are summarized in Table 1, in which the results of $p(\hat{y}|\mathbf{x})$, entropy of $p(y|\mathbf{x})$, Mahalanobis distance and likelihood ratio are from [27]. Results of VIB and NIB are obtained on our test environment with authors’ original code.

5.2 Density Estimation

Now we show how density estimation performance of SGM. We extend the MoG example for mutual information estimations to a generalized mixtures. We randomly assign each

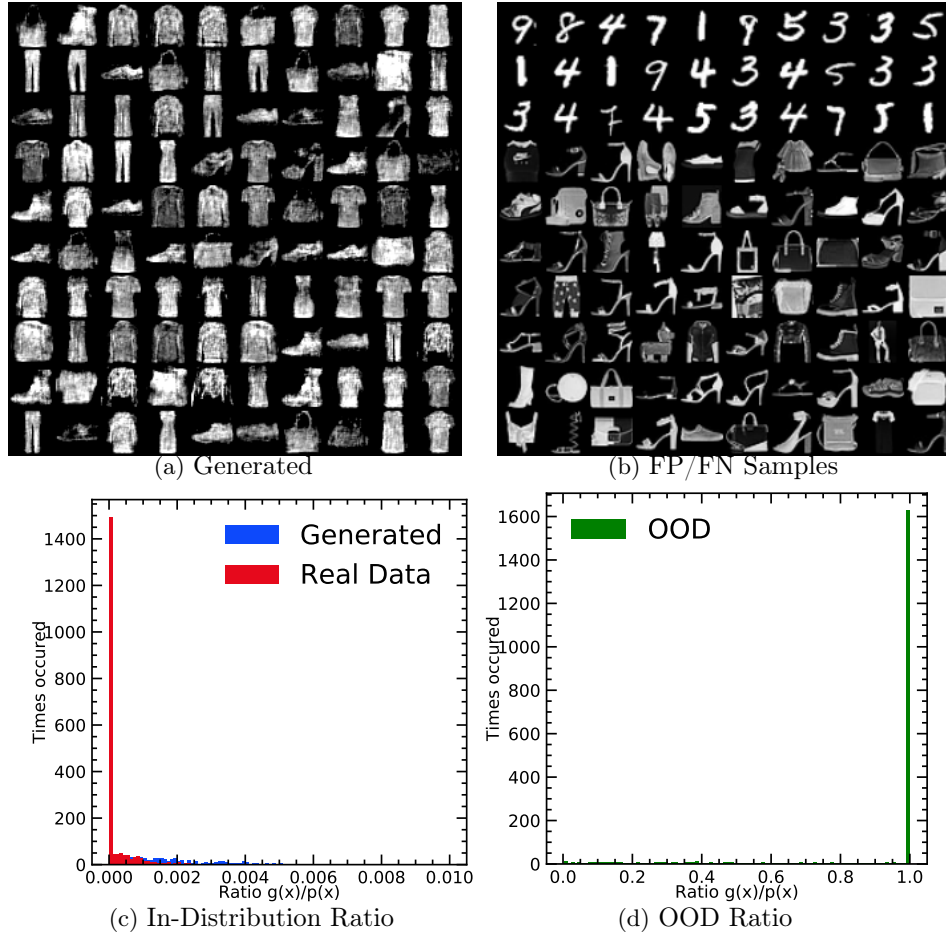


Figure 2: Network outputs trained by (21). (a) shows the generated samples. (b) shows the FP and FN samples when the ratio is set to 10^{-2} . (c) and (c) show the produced probability ratio by the discriminator network for generated data, Fashion MNIST test set, and MNIST test set.

Method	AUROC \uparrow	AUPRC \uparrow	FPR80 \downarrow
Density ratio (ours)	0.997	0.997	0.004
$p(\hat{y} \mathbf{x})$	0.734	0.702	0.506
Entropy of $p(y \mathbf{x})$	0.746	0.726	0.448
Mahalanobis distance	0.942	0.928	0.088
Likelihood ratio	0.994	0.993	0.001
VIB	0.906	0.903	0.172
NIB	0.916	0.913	0.152

Table 1: AUROC \uparrow , AUPRC \uparrow , and FPR (80%TPR) \downarrow for detecting OOD inputs with density ratio and other baselines on Fashion-MNIST vs. MNIST datasets. \uparrow indicates that larger value is better, \downarrow indicates that lower value is better.

center with a Gaussian distribution, a Laplacian distribution, or a uniform distribution. We sample the scale of the Laplacian from $U(0.01, 0.2)$, the subinterval length of each uniform distribution from $U(0.01, 0.2)$, and the weighting factor from $U(0.5, 1.5)$. We generate 200k samples in total and repeat the experiment with different parameters for five times. We compare SGM with GMM and VBGMM. VBGMM has the concentration factor 1.

Evaluations. We use $J_p(g_\theta)$ (CE) and the validation rate for evaluation. We compute CE with (10) for GMM, with (12) for SGM and VBGMM. A greater CE indicates a better performance. To address the overfitting issue that is common in GMM, suppose $m'(j)$ is the j -th true center, we use the validation rate $VR = \mathbb{E}[\mathbf{w} \cdot \mathbb{1}((\min_j \|\mathbf{m}(x_t) - m'(j)\|_2^2) < d)] / \mathbb{E}[\mathbf{w}]$ to calculate the percentage of the components whose mean's distance to the closet true center mass is under $d = 10^{-4}$ or 10^{-2} .

Performance. Table 2 shows that the performance of SGM is higher than both GMM and VBGMM. If we estimate CE's upper bound (14) with the true pdf by subintervals, we obtain 6.68, 21.0, 12.5, 7.26 and 8.25. Since only finite samples are given, the true values are higher. Although VBGMM has a better concentration, it introduces a huge bias regarding performance. With d chosen to be 10^{-2} , all the means of SGM are valid while GMM suffers from severe overfitting, illustrated as Figure 3.

5.3 Modeling Conditional Probabilities

Next we show that SGM is capable of modeling conditional probabilities. We assume that the conditional is given by an artificial continuous-state-space Markov chain. We create a 10×10 matrix with main diagonals to be 0.7 and the other entries to be $1/30$. Then we shuffle the matrix along the x axis and put Gaussian distributions on top of each center, with diagonal covariance matrices sampled from $U(0.0005, 0.002)$ to formulate the single transition probability as $p(x_{t+1}|x_t) = p(x_t, x_{t+1}) / \int_{\mathcal{X}} p(x_t) d\mu$. We start with sampling 100 points from a uniform distribution between 0 and 1. Then we generate trajectories with a length of 1000. In other words, samples will have a joint distribution $p(x, y) = p(x)p(x_{t+1} = y|x_t = x)$ with the marginal $p(x) = \mathbb{E}_{x_0}[\frac{1}{T} \sum_{t=0}^T p(x_t = x)]$.

Evaluations. We compare SGM with GMM, VBGMM, MDN and conditional GAN (CGAN). For GMM and VBGMM, we estimate the joint $p(x, y)$ as described and then marginalize x to obtain $p(y|x) = p(x, y) / \int_{\mathcal{X}} p(x, y) d\mu$. For MDN we use the implementation in [5]. We also implement CGAN [31]. Given two pairs $\{x_t, x_{t+1}\}$ and $\{x'_t, x'_{t+1}\}$, the discriminator tries to distinguish between $\{x_t, g_\theta(x_t)\}$ and $\{x'_t, x'_{t+1}\}$. SGM is trained by (15). For GMM and VBGMM, suppose the covariance matrices are diagonal, notice that $g_\theta(y|x) = \frac{\sum_{j=1}^N w_j \mathcal{N}(x - \mu_{x_j}, \sigma_{x_j}) \mathcal{N}(y - \mu_{y_j}, \sigma_{y_j})}{\sum_{i=1}^N w_i \mathcal{N}(x - \mu_{x_i}, \sigma_{x_i})}$. So we first compute the responsibility for each $x \sim p$, then we compute $J_{Y|X}(g_\theta)$ with (15).

Performance. Figure 4 shows the performance of each method. We find that similar to GMM, MDN also has the tendency to overestimate tail. Since the original joint distribution is a MoG, VBGMM is the most competitive but still has visible bias. For CGAN, we use the empirical estimator to produce the joint distribution as Figure 4g and the conditional as Figure 4h. Since CGAN does not assume the shape of the distribution and its input noise is uniformly distributed, the estimation will always have a bias. Table 3 shows the

Algorithm	CE				
	EXP #1	EXP #2	EXP #3	EXP #4	EXP #5
GMM	6.40	17.31	13.36	7.14	8.06
VBGMM	4.13	4.86	4.33	4.19	5.48
SGM	6.64	18.02	13.80	7.76	9.69
VR $d = 10^{-4}$					
	EXP #1	EXP #2	EXP #3	EXP #4	EXP #5
GMM	0.0036	0.018	0.012	0.015	0.23
VBGMM	0.74	0.84	0.84	0.71	0.89
SGM	0.57	0.24	0.40	0.36	0.37
VR $d = 10^{-2}$					
	EXP #1	EXP #2	EXP #3	EXP #4	EXP #5
GMM	0.86	0.91	0.87	0.61	1.0
VBGMM	1.0	1.0	1.0	1.0	1.0
SGM	1.0	1.0	1.0	1.0	1.0

Table 2: Performance of the 2D density estimation. Although VBGMM has a better concentration, it suffers from a much higher bias compared to vanilla GMM and SGM.

overall score evaluated with CE.

6 Conclusion

This paper presents a novel framework for generative modeling, named SGM, exploiting the nice properties of Rényi’s information in estimation. Since mixtures of Gaussians can be estimated in closed-form by Rényi’s quadratic information, we derive two new cost functions that substitute the cross-entropy and the KL divergence by the corresponding Rényi’s formulations. We then proceed to train a neural network that directly yields a

Algorithm	CE				
	EXP #1	EXP #2	EXP #3	EXP #4	EXP #5
CGAN	0.788	0.796	0.675	0.659	0.887
GMM	0.900	0.939	0.878	0.957	0.980
VBGMM	0.959	0.942	0.904	0.945	0.951
MDN	0.967	0.957	0.889	0.913	0.912
SGM	0.993	0.968	0.923	0.972	0.990

Table 3: Performance for conditional probability modeling.

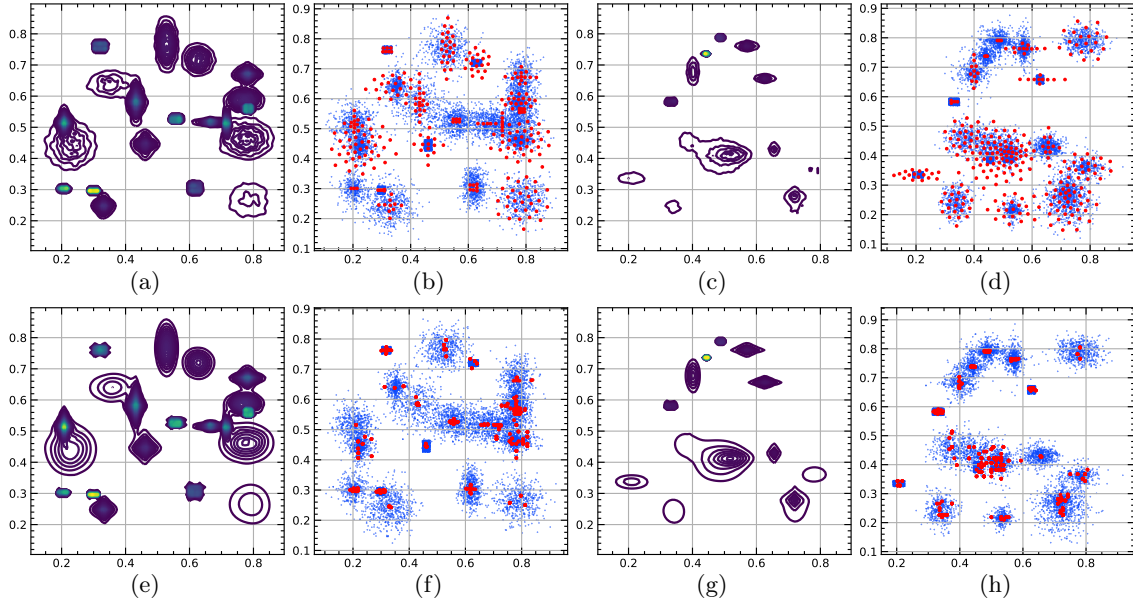


Figure 3: (a) to (d) show the density and model mean components learned by GMM. (e) to (h) show the same figures produced by SGM. The red dots represent the model means and the blue dots represent the data. SGM has a much better performance regarding tail.

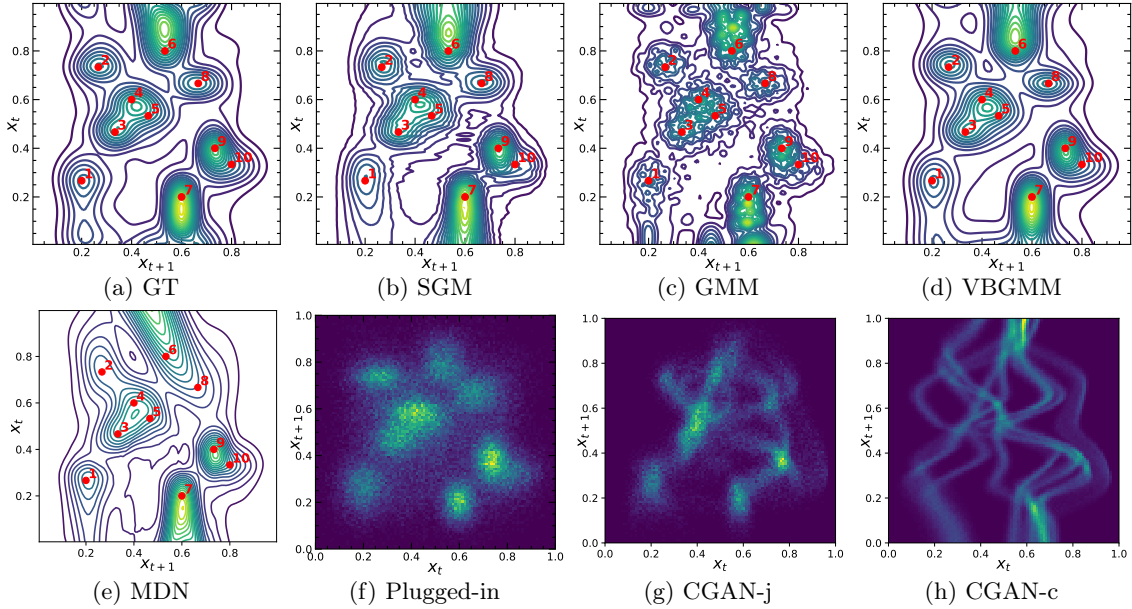


Figure 4: Comparisons of learned transition probabilities. The red dots show the transition with the highest probability at each state when constructing the Markov chain. (g) shows the joint distribution learned by CGAN. (h) shows $p(x_{t+1}|p_t)$ by taking the network input to be evenly spaced between 0 and 1.

generative model of the input data by local approximations of mean and variance in the data space, e.g., under an infinite Gaussian mixture model assumption. This avoids the issue of using bounds (upper or lower) in the conventional generative modeling approaches, which requires assumptions that are very difficult to fulfill in parametric density modeling. The proposed SGM is data-efficient unlike the conventional approaches as we clearly show with the comparison with MINE. In the experiments, we verified the accuracy of the proposed SGM approach. Further work will be directed towards finding alternate approximations to $T(x)$, which will scale better for high dimensions, and extend the method to alpha close to 1 to estimate Shannon information.

References

- [1] José C. Príncipe. *Information theoretic learning: Rényi's entropy and kernel perspectives*. Springer Science & Business Media, 2010.
- [2] Luis Gonzalo Sanchez Giraldo, Murali Rao, and José C Príncipe. Measures of entropy from data using infinitely divisible kernels. *IEEE Transactions on Information Theory*, 61(1):535–548, 2014.
- [3] Shujian Yu, Luis Gonzalo Giraldo, and José C Príncipe. Information-theoretic methods in deep neural networks: Recent advances and emerging opportunities. In *International Joint Conference on Artificial Intelligence*, pages 4669–4678, Survey Track, 2021.
- [4] Yves Grandvalet and Yoshua Bengio. Semi-supervised learning by entropy minimization. In *Proceedings of the 17th International Conference on Neural Information Processing Systems*, pages 529–536, 2004.
- [5] Christopher M Bishop. Mixture density networks. Technical report, 1994.
- [6] XuanLong Nguyen, Martin J Wainwright, and Michael I Jordan. On surrogate loss functions and f-divergences. *The Annals of Statistics*, 37(2):876–904, 2009.
- [7] XuanLong Nguyen, Martin J Wainwright, and Michael I Jordan. Estimating divergence functionals and the likelihood ratio by convex risk minimization. *IEEE Transactions on Information Theory*, 56(11):5847–5861, 2010.
- [8] Ian J Goodfellow, Jean Pouget-Abadie, Mehdi Mirza, Bing Xu, David Warde-Farley, Sherjil Ozair, Aaron Courville, and Yoshua Bengio. Generative adversarial networks. In *Advances in Neural Information Processing Systems*, pages 2672–2680, 2014.
- [9] David M Blei, Alp Kucukelbir, and Jon D McAuliffe. Variational inference: A review for statisticians. *Journal of the American statistical Association*, 112(518):859–877, 2017.
- [10] Carl Edward Rasmussen et al. The infinite gaussian mixture model. In *Advances in Neural Information Processing Systems*, volume 12, pages 554–560, 1999.

- [11] Yingzhen Li and Richard E Turner. Rényi divergence variational inference. In *Proceedings of the 30th International Conference on Neural Information Processing Systems*, pages 1081–1089, 2016.
- [12] Martin Arjovsky, Soumith Chintala, and Léon Bottou. Wasserstein generative adversarial networks. In *International Conference on Machine Learning*, pages 214–223, 2017.
- [13] Sebastian Nowozin, Botond Cseke, and Ryota Tomioka. f-gan: training generative neural samplers using variational divergence minimization. In *International Conference on Neural Information Processing Systems*, pages 271–279, 2016.
- [14] Liam Paninski. Estimation of entropy and mutual information. *Neural Computation*, 15(6):1191–1253, 2003.
- [15] John Paisley, David Blei, and Michael I. Jordan. Variational bayesian inference with stochastic search. *International Conference on Machine Learning*, 2012.
- [16] Diederik P Kingma and Max Welling. Auto-encoding variational bayes. *International Conference on Learning Representations*, 2013.
- [17] Alfréd Rényi. On measures of entropy and information. In *Proceedings of the Fourth Berkeley Symposium on Mathematical Statistics and Probability, Volume 1: Contributions to the Theory of Statistics*. The Regents of the University of California, 1961.
- [18] Kittipat Kampa, Erion Hasanbelliu, and José C Príncipe. Closed-form cauchy-schwarz pdf divergence for mixture of gaussians. In *International Joint Conference on Neural Networks*, pages 2578–2585, 2011.
- [19] Dan Hendrycks and Kevin Gimpel. A baseline for detecting misclassified and out-of-distribution examples in neural networks. In *International Conference on Learning Representations*, 2017.
- [20] Chi Jin, Yuchen Zhang, Sivaraman Balakrishnan, Martin J Wainwright, and Michael I Jordan. Local maxima in the likelihood of gaussian mixture models: Structural results and algorithmic consequences. *Advances in Neural Information Processing Systems*, pages 4123–4131, 2016.
- [21] Jean-Baptiste Hiriart-Urruty and Claude Lemaréchal. *Fundamentals of convex analysis*. Springer Science & Business Media, 2004.
- [22] Mohamed Ishmael Belghazi, Aristide Baratin, Sai Rajeshwar, Sherjil Ozair, Yoshua Bengio, Aaron Courville, and Devon Hjelm. Mutual information neural estimation. In *International Conference on Machine Learning*, pages 531–540, 2018.
- [23] Alfred Rényi. Some fundamental questions of information theory. *Selected Papers of Alfred Renyi*, 2(174):526–552, 1976.

- [24] Bo Hu and José C. Príncipe. Training a bank of wiener models with a novel quadratic mutual information cost function. In *International Conference on Acoustics, Speech and Signal Processing*, pages 3150–3154, 2021.
- [25] Mohamed Ishmael Belghazi, Aristide Baratin, Sai Rajeshwar, Sherjil Ozair, Yoshua Bengio, Aaron Courville, and Devon Hjelm. Mutual information neural estimation. In *International Conference on Machine Learning*, pages 531–540, 2018.
- [26] Robert Jenssen, Jose C Principe, Deniz Erdogmus, and Torbjørn Eltoft. The cauchy-schwarz divergence and parzen windowing: Connections to graph theory and mercer kernels. *Journal of the Franklin Institute*, 343(6):614–629, 2006.
- [27] Jie Ren, Peter J. Liu, Emily Fertig, Jasper Snoek, Ryan Poplin, Mark Depristo, Joshua Dillon, and Balaji Lakshminarayanan. Likelihood ratios for out-of-distribution detection. In *Advances in Neural Information Processing Systems*, volume 32, 2019.
- [28] Kimin Lee, Kibok Lee, Honglak Lee, and Jinwoo Shin. A simple unified framework for detecting out-of-distribution samples and adversarial attacks. In *Neural Information Processing Systems*, 2018.
- [29] Alexander A Alemi, Ian Fischer, and Joshua V Dillon. Uncertainty in the variational information bottleneck. In *UAI Uncertainty in Deep Learning Workshop*, 2018.
- [30] Artemy Kolchinsky, Brendan D Tracey, and David H Wolpert. Nonlinear information bottleneck. *Entropy*, 21(12):1181, 2019.
- [31] Mehdi Mirza and Simon Osindero. Conditional generative adversarial nets. *arXiv preprint arXiv:1411.1784*, 2014.
- [32] Tim Salimans, Andrej Karpathy, Xi Chen, and Diederik P Kingma. Pixelcnn++: Improving the pixelcnn with discretized logistic mixture likelihood and other modifications. In *International Conference on Learning Representations*, 2017.

Supplementary Material

A Implementations

We first state that the codes for the experiments can be found at <https://github.com/bohu615/structured-generative-modeling>. Here we present the network structures we use across the experiments. Table 4 shows the network structure for SGM. We assume the base of the log is 2 for Rényi’s descriptors and e for Shannon’s descriptors. The critical hyperparameters include:

- hidden: the number of the hidden units. We choose the hidden=1024 for MI estimation, density estimation and conditional density estimation.

- `hidden_avg`: the number of the hidden units in the final linear and average pooling layer. Since both $T_0(x) = \beta p(x)$ (density) and $T_0(x) = \beta p(x)/q(x)$ (density ratio) require $T_0(x) > 0$, and the variance produced by SGM should also be non-negative, we find adding an average pooling layer stabilizes and improves the overall results. We choose `hidden_avg=128` or `hidden_avg=1024` for the best results.
- minimum variance σ_0 : we add a small constant to the variance component produced by SGM (the output of `avgpool_v`). We choose $\sigma_0 = 10^{-3}$ for MI estimation when there are 10 or 50 samples, and $\sigma_0 = 10^{-5}$ for the other experiments.

Table 4: Network structure of SGM.

Layer	Previous Layer	Input Size	Output Size
Input	-	-	bs×rand
fc1/ReLU/bn1	Input	bs×rand	bs×hidden
fc2/ReLU/bn2	bn1	bs×hidden	bs×hidden
fc3_m/ReLU	bn2	bs×hidden	bs×hidden
fc4_m/Sigmoid	fc3_m/ReLU	bs×hidden	bs×hidden_avg
avgpool_m	fc4_m/Sigmoid	bs×hidden_avg	bs×output_dim
fc3_v/ReLU	bn2	bs×hidden	bs×hidden
fc4_v/Sigmoid	fc3_v/ReLU	bs×hidden	bs×hidden_avg
avgpool_v	fc4_v/Sigmoid	bs×hidden_avg	bs×output_dim
fc3_w/ReLU	bn2	bs×hidden	bs×hidden
fc4_w/Sigmoid	fc3_w/ReLU	bs×hidden	bs×hidden_avg
avgpool_w	fc4_w/Sigmoid	bs×hidden_avg	bs×output_dim

Table 5 shows the convolutional network when we train a GAN with the proposed cost function. Each “ResidualBlock” contains a convolution layer, an upsampling layer and a batch normalization layer, shown as Table 6. Each convolution layer has the kernel size 1, stride 1 and padding 1, which means it does not change the shape of the input tensor. This structure is consistent with Wasserstein-GAN [12].

Table 5: Network structure of the generator network.

Layer	Previous Layer	Input Size	Output Size
Input	-	-	bs×rand
Linear	Input	bs×rand	bs×2048
Reshape	Linear	bs×2048	bs×128×4×4
ResidualBlock-up1	Reshape	bs×128×4×4	bs×128×8×8
ResidualBlock-up2	up1	bs×128×8×8	bs×128×16×16
ResidualBlock-up3	up2	bs×128×16×16	bs×128×32×32
bn/ReLU/Conv	up3	bs×128×32×32	bs×128×32×32
ReLU/Clamp(0,1)	Conv	bs×128×32×32	bs×128×32×32

Table 6: Structure of each “ResidualBlock”.

Layer	Previous Layer	Input Size	Output Size
Input	-	-	$bs \times 128 \times dim \times dim$
upsample/Conv1	Input	$bs \times 128 \times dim \times dim$	$bs \times 128 \times 2dim \times 2dim$
bn1/ReLU/Conv2	Input	$bs \times 128 \times dim \times dim$	$bs \times 128 \times dim \times dim$
bn2/ReLU/upsample/Conv3	Conv2	$bs \times 128 \times dim \times dim$	$bs \times 128 \times 2dim \times 2dim$
Sum	Conv1&Conv3	$bs \times 128 \times 2dim \times 2dim$	$bs \times 128 \times 2dim \times 2dim$

Table 7b shows the network structure we use for training MINE and Rényi’s MI. For fair comparison, the network architecture is consistent with SGM. We also use this network as the discriminator network when training GAN. For OOD detection, the baselines of using class distribution, entropy of class distribution, Mahalanobis distance and likelihood ratio are obtained from [27] based on PixelCNN++ [32], where the authors also uses the notMNIST dataset¹ for hyperparameter tuning. We use open-source codes for VIB² and NIB³ implementations. For conditional density estimation, the implementations of MDN⁴, CGAN⁵, VBGMM⁶ follow the open-source codes available online.

Table 7: Network structure of MINE.

Layer	Previous Layer	Input Size	Output Size
Input	-	-	$bs \times rand$
fc1/ReLU/bn1	Input	$bs \times rand$	$bs \times hidden$
fc2/ReLU/bn2	bn1	$bs \times hidden$	$bs \times hidden$
fc3/ReLU	bn2	$bs \times hidden$	$bs \times hidden$
fc4/Sigmoid	fc3/ReLU	$bs \times hidden$	$bs \times hidden_avg$
avgpool	fc4/Sigmoid	$bs \times hidden_avg$	$bs \times output_dim$

B Details of SGM

We provide pseudo codes for SGM implementations. The main algorithm for density estimation is given as Algorithm 1, where N is the number of discrete components and M is the chosen batch size. For the adaptive updates, we choose $\beta_1 = 0.999$ for v_t and $\beta_2 = 0.9$ for c_t .

For simplification, we denote the adaptive updates from line 10 to line 12 as $\hat{v}_t = ADP(v'_t, t)$ and $\hat{c}_t = ADP(c'_t, t)$. Assuming we want to model the conditional of Y given X , Algorithm 2 shows the procedure for modeling conditional distribution. We further simplify the pair-wise

¹<http://yaroslavvb.blogspot.com/2011/09/notmnist-dataset.html>

²https://github.com/makezur/VIB_pytorch

³<https://github.com/artemyk/nonlinearIB>

⁴<https://github.com/sagelywizard/pytorch-mdn>

⁵<https://github.com/eriklindernoren/PyTorch-GAN>

⁶<https://scikit-learn.org/stable/modules/mixture.html>

Algorithm 1 SGM for Density Estimation

```

1: Initialize  $c_0 \leftarrow 0$ ;  $v_0 \leftarrow 0$ ;  $t \leftarrow 0$ ; Initialize  $\theta_0$ 
2: while  $\theta_t$  not converge do
3:    $t \leftarrow t + 1$ 
4:   Sample  $\{c_1, c_2, \dots, c_M\}$  from  $U(0, 1)$ ; Sample  $\{x_1, x_2, \dots, x_M\}$  from data distribution
5:   for  $i = 1, 2 \dots N$  and  $j = 1, 2 \dots M$  do
6:      $w_{i,j} = f_{\theta_{t-1}}^{(w)}(z_i, c_j)$ ;  $m_{i,j} = f_{\theta_{t-1}}^{(m)}(z_i, c_j)$ ;  $A_{i,j} = f_{\theta_{t-1}}^{(A)}(z_i, c_j)$ 
7:   end for
8:    $v'_t = \frac{1}{M^2 N^2} \sum_{i,j=1}^{N,M} \sum_{i',j'=1}^{N,M} w_{i,j} w_{i',j'} \mathcal{N}(m_{i,j} - m_{i',j'}, A_{i,j} + A_{i',j'})$ 
9:    $c'_t = \frac{1}{MN^2} \sum_{i,j=1}^{N,M} \sum_{j'=1}^M w_{i,j} \mathcal{N}(m_{i,j} - x_{j'}, A_{i,j})$ 
10:   $v_t = \beta_1 \cdot v_{t-1} + (1 - \beta_1) \cdot v'_t$ 
11:   $\hat{v}_t = v_t / (1 - \beta_1^t)$ 
12:   $c_t = \beta_2 \cdot c_{t-1} + (1 - \beta_2) c'_t$ 
13:   $\hat{c}_t = c_t / (1 - \beta_2^t)$ 
14:   $\theta_t = \theta_{t-1} + r \left( \frac{\partial c'_t}{\partial \theta_t} / \sqrt{\hat{v}_t} - \frac{1}{2} (\hat{c}_t \frac{\partial v'_t}{\partial \theta_t}) / \sqrt{\hat{v}_t^3} \right)$ 
15: end while
16: Compute  $\hat{H}_2(p) = -2 \log(\hat{c}_t / \sqrt{\hat{v}_t})$ 

```

computation as

$$\text{Cross}(\{x_i\}_{i=1}^M, \{m_i, w_i, A_i\}_{i=1}^M) = \frac{1}{M} \sum_{i=1}^M w_i \mathcal{N}(m_i - x_i, A_i). \quad (22)$$

Then Algorithm 3 shows the procedure of using SGM for MI estimation. The main algorithm is similar to Algorithm 1 with the task to estimate the joint $p(x, y)$. As the model distribution approaches the joint, the term $\hat{I}_Q = -\frac{1}{2} \log(\frac{\hat{c}_2 \hat{c}_3}{\hat{c}_1 \hat{c}_4})$ becomes an unbiased estimator of the QMI $I_Q = -\log \langle p(x, y), p(x)p(y) \rangle + \frac{1}{2} \log \langle p(x)p(y), p(x)p(y) \rangle + \frac{1}{2} \log \langle p(x, y), p(x, y) \rangle$ as shown in the paper. We use $\text{Shuffle}(\cdot)$ as shuffling the inputs or the parameters to sample from the marginal. We assume both x and y are K -dimensional. We shuffle the first K entries and the second K entries of $\{m_i, w_i, A_i\}_{i=1}^M$ respectively to produce $\{m'_i, w'_i, A'_i\}_{i=1}^M$.

C Closed-form Solution of Rényi's Information Descriptors

The underlying theory for this section is explained in Chapter 2 of [1]. Here we just give a brief review. This paper addresses the special connections between Rényi's Information descriptors and the properties of MoG:

$$\begin{aligned} \int_{\mathcal{X}} T_{\varphi}^2(x) d\mu &= \sum_{i=1}^N \sum_{j=1}^N w_i w_j \mathcal{N}(m_i - m_j, A_i + A_j) \quad \text{for MoG,} \\ \int_{\mathcal{X}} T_{\varphi}^2(x) d\mu &= \mathbb{E}_{\varphi_1 \sim P_{\varphi}, \varphi_2 \sim P_{\varphi}} [\mathbf{w}_1 \mathbf{w}_2 \mathcal{N}(\mathbf{m}_1 - \mathbf{m}_2, \mathbf{A}_1 + \mathbf{A}_2)] \quad \text{for IMoG.} \end{aligned} \quad (23)$$

Algorithm 2 SGM for Conditional Distribution Modeling

```
1: Initialize  $c_0 \leftarrow 0$ ;  $v_0 \leftarrow 0$ ;  $t \leftarrow 0$ ; Initialize  $\theta_0$ 
2: while  $\theta$  not converge do
3:    $t \leftarrow t + 1$ 
4:   Sample  $\{c_1, \dots, c_M\}$  and  $\{c'_1, \dots, c'_M\}$  from  $U(0, 1)$ 
5:   Sample  $\{z_1, \dots, z_M\}$  and  $\{z'_1, \dots, z'_M\}$  from  $\text{Cat}(N)$ 
6:   Sample  $\{\{x_1, y_1\}, \dots, \{x_M, y_M\}\}$  from data distribution
7:   for  $i = 1, 2 \dots M$  do
8:      $w_i = f_{\theta_{t-1}}^{(w)}(z_i, c_i; x_i)$ ;  $m_i = f_{\theta_{t-1}}^{(m)}(z_i, c_i; x_i)$ ;  $A_i = f_{\theta_{t-1}}^{(A)}(z_i, c_i; x_i)$ 
9:      $w'_i = f_{\theta_{t-1}}^{(w)}(z'_i, c'_i; x_i)$ ;  $m'_i = f_{\theta_{t-1}}^{(m)}(z'_i, c'_i; x_i)$ ;  $A'_i = f_{\theta_{t-1}}^{(A)}(z'_i, c'_i; x_i)$ 
10:   end for
11:    $v'_t = \frac{1}{M} \sum_{i=1}^M w_i w_{i'} \mathcal{N}(m_i - m_{i'}, A_i + A_{i'})$ 
12:    $c'_t = \frac{1}{2M} \left( \sum_{i=1}^M w_i \mathcal{N}(m_i - y_i, A_i) + \sum_{i=1}^M w'_i \mathcal{N}(m'_i - y_i, A'_i) \right)$ 
13:    $\hat{v}_t = \text{ADP}(v'_t, t)$ ,  $\hat{c}_t = \text{ADP}(c'_t, t)$ 
14:    $\theta_t = \theta_{t-1} + r \left( \frac{\partial c'_t}{\partial \theta_t} / \sqrt{\hat{v}_t} - \frac{1}{2} (\hat{c}_t \frac{\partial v'_t}{\partial \theta_t}) / \sqrt{\hat{v}_t^3} \right)$ 
15: end while
16: Compute  $\hat{H}_2(Y|X) = -2 \log(\hat{c}_t / \sqrt{\hat{v}_t})$ 
```

Algorithm 3 SGM for MI Estimation

```
1: while at each time  $t$  do
2:    $\{x'_i\}_{i=1}^M = \text{Shuffle}(\{x_i\}_{i=1}^M)$ ,  $\{y'_i\}_{i=1}^M = \text{Shuffle}(\{y_i\}_{i=1}^M)$ 
3:    $\{m'_{i,:K}, w'_{i,:K}, A'_{i,:K}\}_{i=1}^M = \text{Shuffle}(\{m_{i,:K}, w_{i,:K}, A_{i,:K}\}_{i=1}^M)$ 
4:    $\{m'_{i,K}, w'_{i,K}, A'_{i,K}\}_{i=1}^M = \text{Shuffle}(\{m_{i,K}, w_{i,K}, A_{i,K}\}_{i=1}^M)$ 
5:    $\{m'_i, w'_i, A'_i\}_{i=1}^M = \{\{m'_{i,:K}, m'_{i,K}\}, \{w'_{i,:K}, w'_{i,K}\}, \{A'_{i,:K}, A'_{i,K}\}\}$ 
6:    $c'_1 = \text{Cross}(\{x_i, y_i\}_{i=1}^M, \{m_i, w_i, A_i\}_{i=1}^M)$ ,  $c'_2 = \text{Cross}(\{x_i, y_i\}_{i=1}^M, \{m'_i, w'_i, A'_i\}_{i=1}^M)$ 
7:    $c'_3 = \text{Cross}(\{x'_i, y'_i\}_{i=1}^M, \{m_i, w_i, A_i\}_{i=1}^M)$ ,  $c'_4 = \text{Cross}(\{x'_i, y'_i\}_{i=1}^M, \{m'_i, w'_i, A'_i\}_{i=1}^M)$ 
8:    $\hat{c}_1 = \text{ADP}(c'_1, t)$ ,  $\hat{c}_2 = \text{ADP}(c'_2, t)$ ,  $\hat{c}_3 = \text{ADP}(c'_3, t)$ ,  $\hat{c}_4 = \text{ADP}(c'_4, t)$ 
9: end while
10: Compute  $\hat{I}_Q(X, Y) = -\log(\frac{\hat{c}_2 \hat{c}_3}{\hat{c}_1 \hat{c}_4})$ 
```

It follows that Rényi's second-order entropy is given as $H_2(T_\varphi) = -\log(\int_{\mathcal{X}} T_\varphi^2(x) d\mu)$. Thus Rényi's second-order entropy has a closed-form solution for MoG and IMoG. In this section, we further provide two more Rényi's information descriptors for MoG and IMoG based on this property.

Divergence. Let two MoG or IMoG T_{φ_1} and T_{φ_2} be given, it's easy to show that

$$\begin{aligned} \int_{\mathcal{X}} T_{\varphi_1}(x) T_{\varphi_2}(x) d\mu &= \sum_{i=1}^{N_1} \sum_{j=1}^{N_2} w_i w'_j \mathcal{N}(m_i - m'_j, A_i + A'_j) \quad \text{for MoG,} \\ \int_{\mathcal{X}} T_{\varphi_1}(x) T_{\varphi_2}(x) d\mu &= \mathbb{E}_{\varphi_1 \sim P_{\varphi_1}, \varphi_2 \sim P_{\varphi_2}} [\mathbf{w}_1 \mathbf{w}_2 \mathcal{N}(\mathbf{m}_1 - \mathbf{m}_2, \mathbf{A}_1 + \mathbf{A}_2)] \quad \text{for IMoG.} \end{aligned} \quad (24)$$

As $J_{T_{\varphi_1}}(T_{\varphi_2}) = \int_{\mathcal{X}} T_{\varphi_1}(x) T_{\varphi_2}(x) d\mu / (\int_{\mathcal{X}} T_{\varphi_2}^2(x) d\mu)^{\frac{1}{2}}$ is defined as the cross-entropy in this paper, it's natural to construct the divergence between T_{φ_1} and T_{φ_2} as

$$\text{csd}(T_{\varphi_1}, T_{\varphi_2}) = \frac{\int_{\mathcal{X}} T_{\varphi_1}(x) T_{\varphi_2}(x) d\mu}{(\int_{\mathcal{X}} T_{\varphi_1}^2(x) d\mu)^{\frac{1}{2}} (\int_{\mathcal{X}} T_{\varphi_2}^2(x) d\mu)^{\frac{1}{2}}}, \quad \text{CSD}(T_{\varphi_1}, T_{\varphi_2}) = -\log \text{csd}(T_{\varphi_1}, T_{\varphi_2}). \quad (25)$$

The relationship $\text{CSD}(T_{\varphi_1}, T_{\varphi_2}) = \log J_{T_{\varphi_1}}(T_{\varphi_2}) + H_2(T_{\varphi_2}) = \log J_{T_{\varphi_2}}(T_{\varphi_1}) + H_2(T_{\varphi_1})$ holds. CSD is the definition of Cauchy-Schwarz divergence [1, 26]. It's easy to show that $\text{csd} \leq 1$ given by the Cauchy-Schwarz inequality. Combining (23) and (24), we state that $\text{CSD}(T_{\varphi_1}, T_{\varphi_2})$ has a closed-form solution that no longer requires the probability ratio.

To further demonstrate the effectiveness of this descriptor, we conduct an additional experiment based on the dataset created for MI estimation, shown as Figure 5a. As two distributions become the same, the value of csd will reach its largest value 1. As two distributions are more and more separated by shifting, the value of csd will trend down and eventually reach 0. Figure 5b shows the change of csd as the distributions get shifted. Similar to estimating MI, SGM has no difficulty of estimating csd , as shown as the red dots in Figure 5b. Note that this problem cannot be solved by MINE or Rényi's second-order divergence since the probability ratio $T_{\varphi_1}/T_{\varphi_2}$ may not exist. For MoG and IMoG where (24) has a much simpler form than the probability ratio, this descriptor shows a huge advantage.

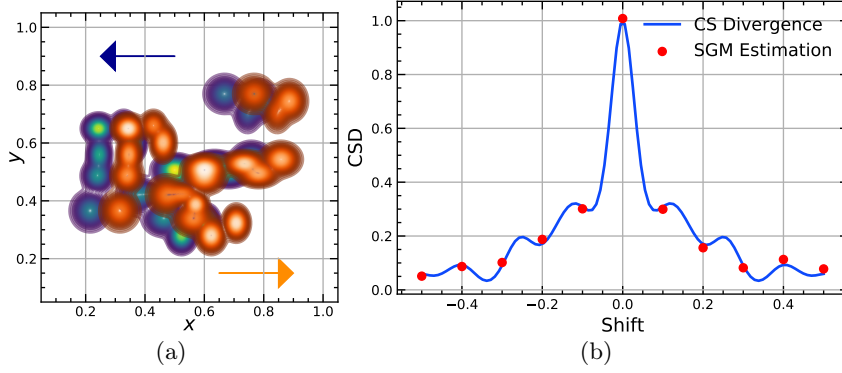


Figure 5: (a) shows the two distributions we use for divergence estimation. As two distributions are more and more separated by shifting, csd is expected to start from 1 and eventually reach 0. (b) shows the closed-form solution computed with (24) and the estimation by SGM. We plot the value of $\text{csd}(T_{\varphi_1}, T_{\varphi_2})$, which is a coefficient between 0 and 1. Therefore it correctly characterizes the divergence between two distributions, and SGM can be easily utilized for estimating this descriptor.

Mutual information. Based on CSD, the closed-form solution for mutual information can easily be given. Suppose the joint distribution of X and Y follows a MoG as $T_{\varphi}(x, y) = \sum_{i=1}^N w_i \mathcal{N}([x, y]^T - \mu_i, A_i)$. It follows that $T_{\varphi}(y) = \int_{\mathcal{X}} T_{\varphi}(x, y) d\mu = \sum_{i=1}^N w_i \mathcal{N}(y - \mu_i^{(2)}, A_i^{(2,2)})$ and $T_{\varphi}(x) = \sum_{i=1}^N w_i \mathcal{N}(x - \mu_i^{(1)}, A_i^{(1,1)})$, where $\mu_i^{(1)}$ and $\mu_i^{(2)}$ are the entries in μ that corresponds to X and Y . The matrices $A_i^{(1,1)}$ and $A_i^{(2,2)}$ are the blocks in A_i that corresponds to X and Y . It follows that $T_{\varphi}(x)T_{\varphi}(y)$ is also a MoG. Therefore we take $\text{QMI}(T_{\varphi}) = \text{CSD}(T_{\varphi}(x)T_{\varphi}(y), T_{\varphi}(x, y))$ as the mutual information, which implies the closed-form solution exists. This is exactly the definition of QMI [1] we use in the MI estimation experiment. The same conclusion can be extended to IMoG.

We use the same example for illustration. Figure 6a to Figure 6d show the corresponding quantities for T_{φ} . It can be seen that for MoG or IMoG, the term $T_{\varphi}(x, y)T_{\varphi}(x)T_{\varphi}(y)$ has a much simpler structure than the probability ratio $\frac{T_{\varphi}(x, y)}{T_{\varphi}(x)T_{\varphi}(y)}$. Therefore using QMI greatly simplifies the computation.

We further illustrate the MI estimation experiments. As stated in the paper, the optimal solution is $T_0 = \beta p(x)/q(x)$ when training with $J_{p,q}(T_{\theta})$. As $J_{p,q}(T_{\theta})$ is used to estimate Rényi’s MI, the network output should approach Figure 6d. Although it is not visualized in the original paper of MINE [22], the authors address that the network output should reach $T_0(x) = \log(p(x)/q(x)) + C$. Suppose T_{θ} is given by MINE, the term $e^{T_{\theta}}$ should reach Figure 6d. The result of using Rényi’s MI is shown as Figure 7a. The result of using MINE is shown as Figure 7b. We should still notice that MINE is still much more unstable and can diverge easily. Rényi’s MI has the best result compared to Figure 6d. Since the product shown in Figure 6c has a much simpler structure, SGM is the most accurate regarding estimating MI, where the approximation of the joint is shown as Figure 7c.

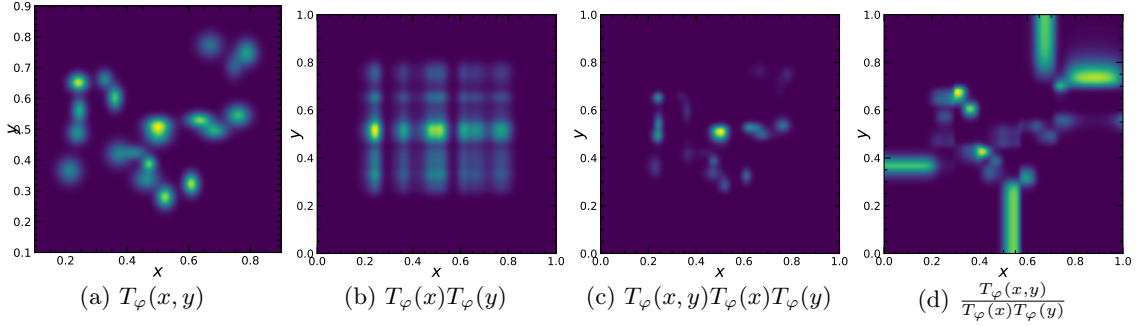


Figure 6: Visualizations of various quantities based on the MI estimation example. While Rényi’s MI and MINE yields the probability ratio in (d), the product term in (c) has a much simpler structure. Therefore approximating QMI with SGM is a better choice in this scenario.

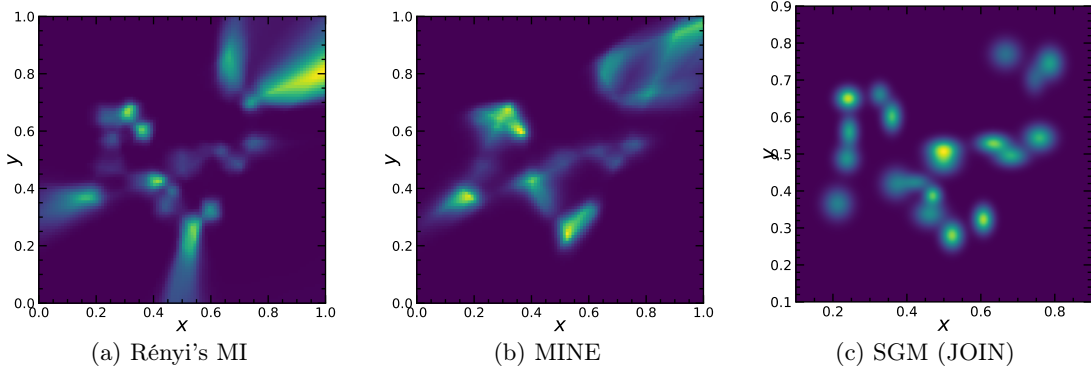


Figure 7: The outputs of the three MI estimators used in the paper. Training with $J_{p,q}(T_\theta)$ yields directly the probability ratio (a). To produce (b) for MINE requires computing e^{T_θ} . MINE will diverge before it learns the tail of the distribution and Rényi’s MI has a higher accuracy compared to Figure 6b. SGM instead produces the joint distribution (c) and the corresponding terms in Figure 6b and Figure 6c, thus it’s the most accurate.

D Additional Experiments for OOD detection

To further show how the training procedure of OOD detection evolves, we visualize the results during training as Figure 8. From the first column to the last column are the results from 1 iteration, 10 iterations, 200 iterations and 4k iterations. Figure 8a to Figure 8d show the generated samples. Figure 8e to Figure 8h show the network output for the generated samples and the train set (Fashion MNIST). Figure 8i to Figure 8l show the network output of the generated samples and the Fashion MNIST test set. Figure 8m to Figure 8p show how the network outputs for OOD samples (MNIST) evolve. Figure 9 show the final results at 100k iterations. This further demonstrates that the network is robust and learns to put only the in-distribution samples in the null space of the network.

E Additional Experiments for Density Estimation

We further visualize all five experiments mentioned in the paper, shown as Figure 10. It can be seen that SGM has a much lower bias and higher accuracy regarding the model centers. Figure 11 shows the training curves of CE for the five experiments, which demonstrates that SGM is stable with a very low variance.

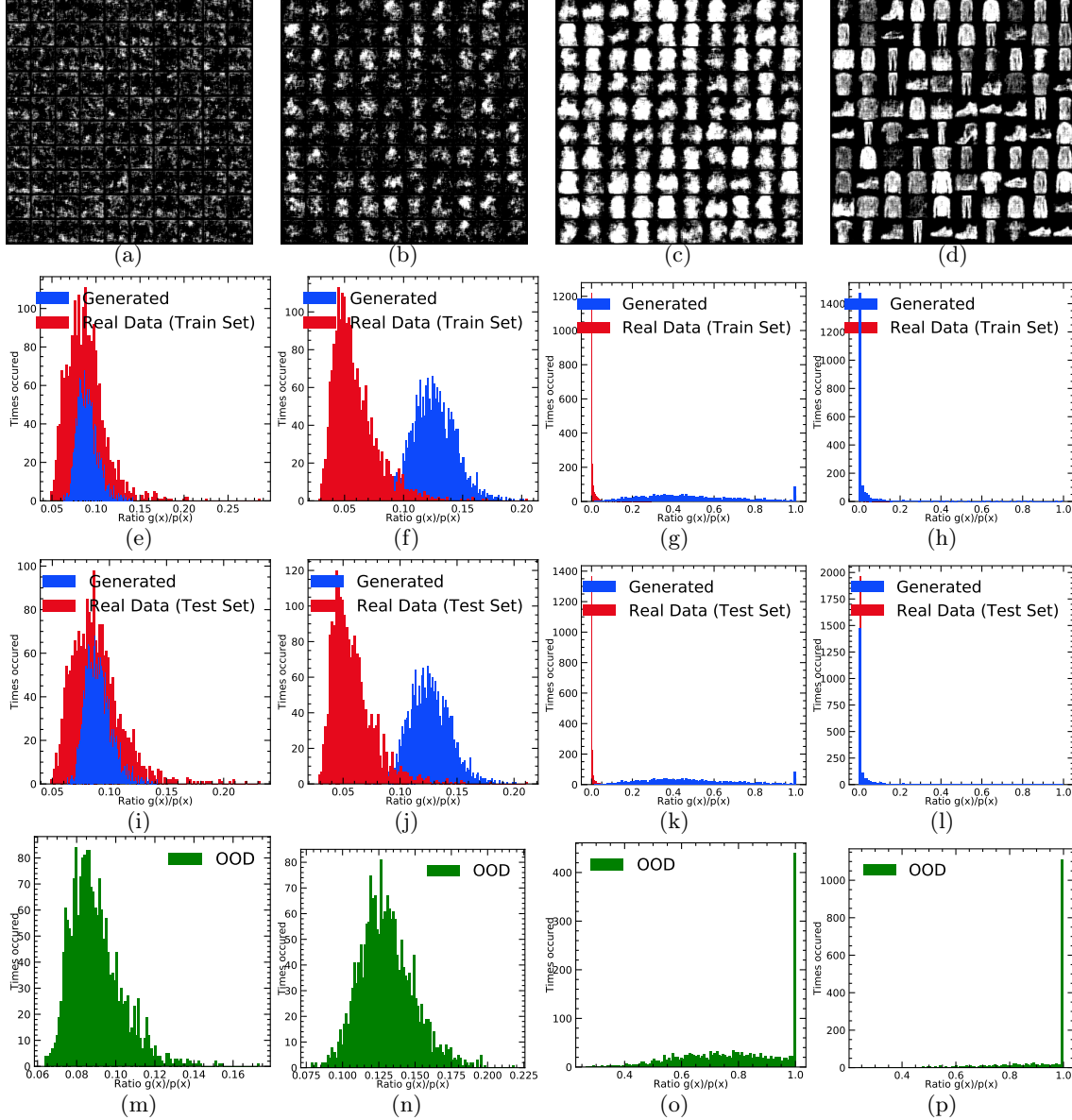


Figure 8: From the left to the right are the visualizations at iteration 1, 10, 200, and 4k. (a) to (d) show the generated samples. (e) to (h) show the network outputs for generated samples and the Fashion MNIST train set. (i) to (l) show the outputs for generated samples and the Fashion MNIST test set. (m) to (p) show the network outputs of OOD samples (MNIST). As the training proceeds, the network learns to put only the in-distribution samples around 0 and the OOD samples around 1.

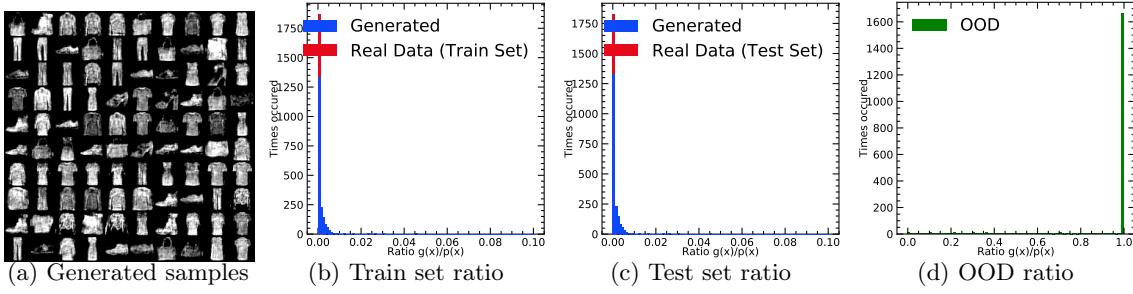


Figure 9: Final results at 100k iterations. Most in-distribution samples and generated samples have ratio values smaller than 0.01 while most OOD samples have values at 1.

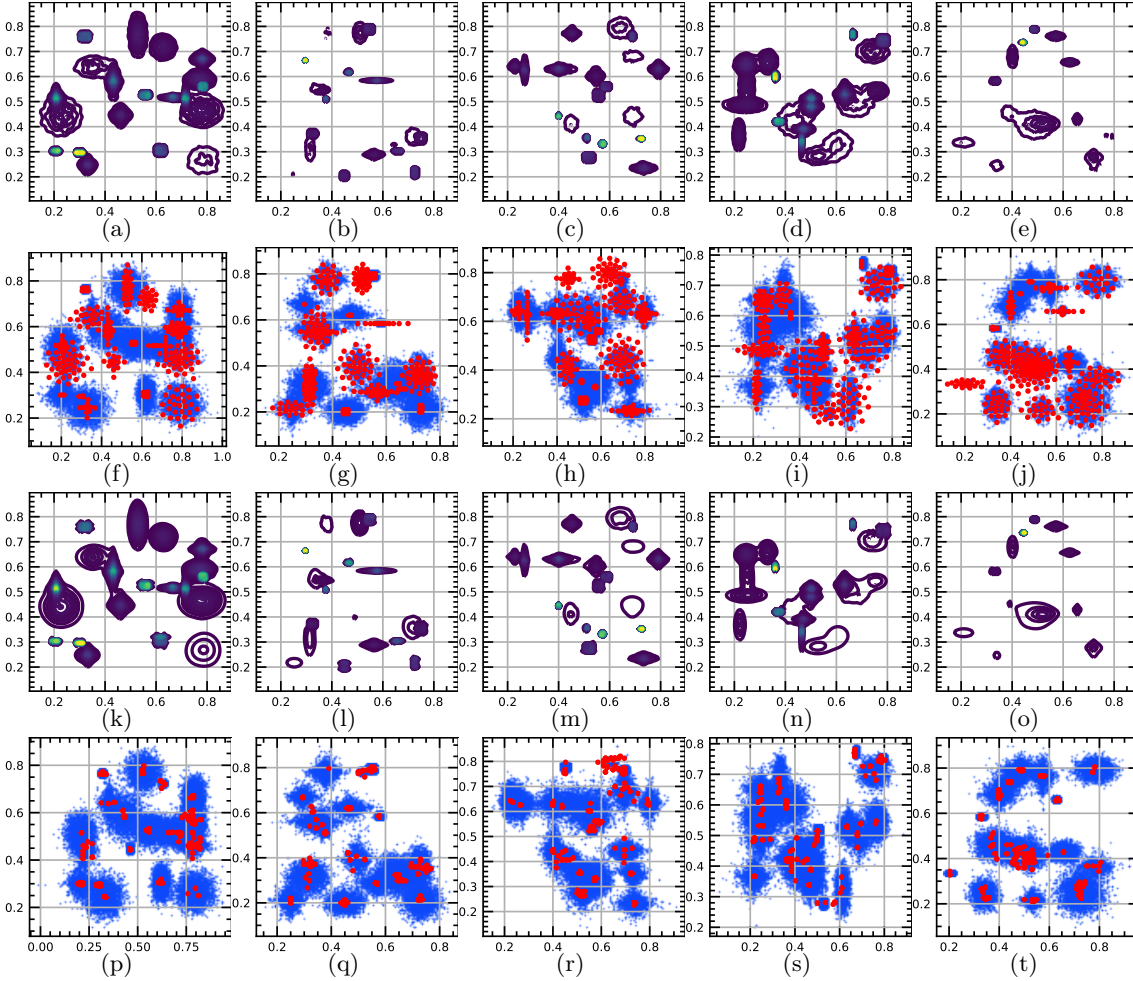


Figure 10: Visualizations of all five experiments for density estimation. (a) to (e) show the densities produced by GMM. (f) to (j) show the model mean components produced by GMM. (k) to (t) show the corresponding figures produced by SGM. It can be seen that all five experiments show that SGM has a much lower bias and a much better concentration regarding the centers.

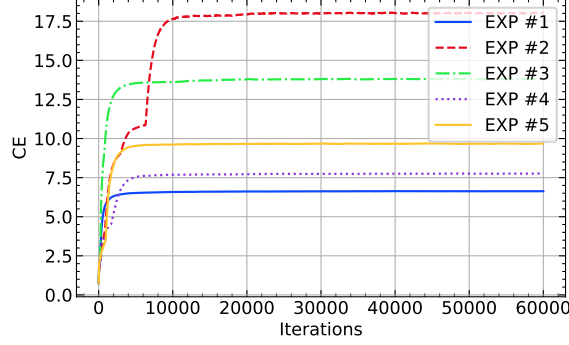


Figure 11: Training curves of CE for density estimation. It demonstrates that SGM is stable with a very low variance. The upper bound given infinite number of samples would be 6.68, 21.0, 12.5, 7.26 and 8.25.

F Understanding GMM’s Overfitting Problem with Absolute Continuity

As described in Section 2 in the paper, GMM suffers from a well-known overfitting issue. EM and variational inference can be said to optimize an upper bound of $\text{CE}(p, g_\theta)$:

$$\begin{aligned} \text{CE}(p, g_\theta) &= \int_{\mathcal{X}} \int_{\mathcal{Z}} p(x) \frac{g_\theta(x, z)}{\int_{\mathcal{Z}} g_\theta(x, z) d\mu} \log \frac{g_\theta(x, z)}{\int_{\mathcal{Z}} g_\theta(x, z) d\mu} d\mu d\mu - \int_{\mathcal{X}} \int_{\mathcal{Z}} p(x) \frac{g_\theta(x, z) \log g_\theta(x, z)}{\int_{\mathcal{Z}} g_\theta(x, z) d\mu} d\mu d\mu \\ &\leq - \int_{\mathcal{X}} \int_{\mathcal{Z}} p(x) (g_\theta(x, z) / g_\theta(x)) \log g_\theta(x, z) d\mu = \text{CE}(p(x)g_\theta(x, z) / g_\theta(x), g_\theta(x, z)). \end{aligned} \quad (26)$$

However, the bound only exists when $p(x) > 0$ implies $g_\theta(x) > 0$, i.e. the Lebesgue measures are absolute continuous. Suppose there exists x such that $p(x) > 0$ and $g_\theta(x) = 0$, the LHS no longer exists while the responsibility $g_\theta(x, z) / g_\theta(x)$ is taken to have finite values for the computation. Therefore the bound no longer holds.

We demonstrate this issue by a short example. We construct a MoG p with two components, each with a variance σ^2 . We fix one component and vary the mean of the other component over the space to create g_θ , then plot $\text{CE}(p, g_\theta)$ and its upper bound. We compute the responsibility with $g_\theta(x, z) / (g_\theta(x) + 10^{-6})$. Figure 12a shows that the upper bound holds only in a small region around the true center. Figure 12b to 12d show fitting GMM with 30 centers, with model centers colored in blue. The heatmap shows the upper bound, where a clear boundary can be seen similar to Figure 12a. The model centers lie in the region where the bound holds.

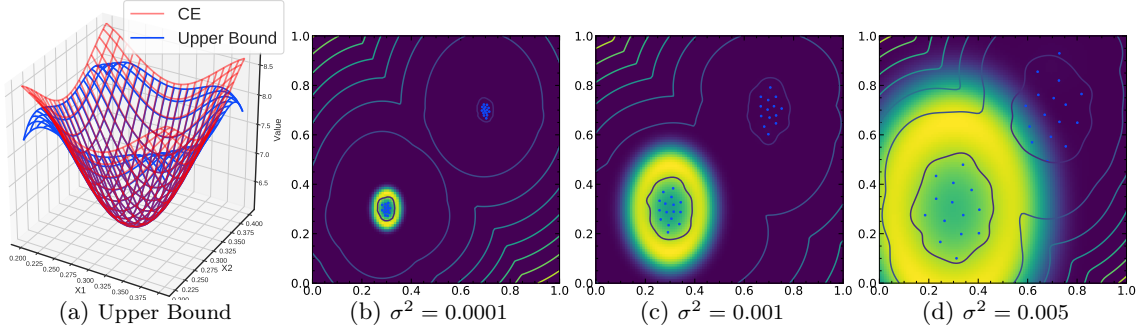


Figure 12: (a) shows the upper bound holds only for a small region around the true center if the responsibility is computed as $g_\theta(x, z)/(g_\theta(x) + 10^{-6})$; (b), (c) and (d) show the model centers scatteredly lie in the region where the upper bound holds. CE in (a) is computed by (26).

This demonstration shows the dangers of using parametric models such as MINE to estimate entropy [22]. Although it is true that cross entropy is an upper bound for entropy, the upper bound such as (26) can be very loose if the two measures are not absolute continuous, and in parametric modeling it is basically impossible to guarantee this condition because of the way the model parameters change. The same reasoning holds for KL divergence and ELBO.

So the conclusion is that machine learning researchers should be more aware of the issue of the absolute continuity, and understand its impact of the looseness of the bounds. Therefore, these estimators should only be used in very well controlled conditions. Alternatively, the family of non-parametric estimators in RKHS is an efficient way to proceed, as demonstrated in this paper.